

Study of Quasi-Monophase Y-Type Hexaferrite $\text{Ba}_2\text{Mg}_2\text{Fe}_{12}\text{O}_{22}$ Powder

Tatyana Koutzarova¹, Svetoslav Kolev¹, Ivan Nedkov¹, Kiril Krezhov², Daniela Kovacheva³, Chavdar Ghelev¹, Bénédicte Vertruyen⁴, Catherine Henrist⁴ and Rudi Cloots⁴

¹*Institute of Electronics, Bulgarian Academy of Sciences, 72 Tsarigradsko Chaussée, 1784 Sofia, Bulgaria;*
²*Institute for Nuclear Research and Nuclear Energy, Bulgarian Academy of Sciences, 72 Tsarigradsko Chaussée, Blvd. 1784 Sofia, Bulgaria;* ³*Institute of General and Inorganic Chemistry, Bulgarian Academy of Sciences, Acad. Georgi Bonchev Str, bid. 11, 1113 Sofia, Bulgaria;* ⁴*LSIC, Chemistry Department B6, University of Liege, Sart Tilman, B-4000 Liege, Belgium*

ABSTRACT: We present the structural and magnetic properties of a multiferroic $\text{Ba}_2\text{Mg}_2\text{Fe}_{12}\text{O}_{22}$ hexaferrite composite containing a small amount of MgFe_2O_4 . The composite material was obtained by auto-combustion synthesis and, alternatively, by co-precipitation. The $\text{Ba}_2\text{Mg}_2\text{Fe}_{12}\text{O}_{22}$ particles obtained by co-precipitation have an almost perfect hexagonal shape in contrast with those prepared by auto-combustion. Two magnetic phase transitions, responsible for the composite's multiferroic properties, were observed, namely, at 183 K and 40 K for the material produced by auto-combustion, and at 196 K and 30 K for the sample prepared by co-precipitation. No magnetic phase transitions in these temperature ranges were observed for a MgFe_2O_4 sample, which shows that the magnesium ferrite does not affect the multiferroic properties of this type of multiferroic materials.

KEYWORDS: Auto-combustion synthesis, $\text{Ba}_2\text{Mg}_2\text{Fe}_{12}\text{O}_{22}$, co-precipitation, MgFe_2O_4 , multiferroic composite, multiferroic properties, Y-type hexaferrite.

1. INTRODUCTION

Multiferroic materials in which long-range magnetic and ferroelectric orders coexist have recently been of great interest in the fields of both basic and applied sciences [1, 2]. In particular, those exhibiting a ferroelectric transition inducing a certain kind of magnetic ordering are of much interest, because in such systems the effects of coupling between magnetism and electric polarization are expected to give rise to new physical phenomena. The interest in these materials has also had to do with their possible applications in next generation electronic devices that make use of the magnetic (spin) state control via electric fields and/or vice versa, with potential for spintronic devices, solid-state transformers, high sensitivity magnetic field sensors, and electromagneto-optic actuators [3].

Most multiferroics exhibit a magnetoelectric effect at low temperatures and applied magnetic fields exceeding 0.1 T that are too high to be of practical use [4]. However, it was found recently that some hexaferrites exhibit magnetoelectric effect at room temperature and a low magnetic field (~ 0.01 T) [5].

The Y-type hexagonal ferrite $\text{Ba}_2\text{Mg}_2\text{Fe}_{12}\text{O}_{22}$ is an example of a multiferroic material. It has a relatively high spiral-magnetic transition temperature (~ 200 K), shows multiferroic properties at zero magnetic field, and the direction of the ferroelectric polarization can be controlled by a weak magnetic field (< 0.02 T) [2]. Moreover, it is an important type of high-frequency soft magnetic material due to its strong planar magnetic anisotropy [6], which, in combination with its high permeability, make it attractive for practical applications in microwave devices [7].

Due to the fact that the Y-type hexaferrites are an intermediate phase during the synthesis of Z-type ferrites, which are suitable for multi-layer chip inductors [8, 9], not much attention has been paid to their synthesis and magnetic properties investigation.

The Y-type $\text{Ba}_2\text{Mg}_2\text{Fe}_{12}\text{O}_{22}$ ferrite is built from a superposition of *T* and *S* blocks along the *c*-axis direction. The unit cell is composed of a sequence of *STSTST* blocks. It has an easy axis of magnetization lying in a plane normal to the *c*-axis direction. $\text{Ba}_2\text{Mg}_2\text{Fe}_{12}\text{O}_{22}$ consists of two magnetic sublattice blocks, *L* and *S* blocks, stacked alternately along the [001] axis, which bear, respectively, the opposite large and small magnetization *M*, causing ferrimagnetism even at high temperatures exceeding room temperature. The Curie point of $\text{Ba}_2\text{Mg}_2\text{Fe}_{12}\text{O}_{22}$ is 553 K. Below 195 K, the spins form a proper screw spin structure with the propagation vector

along the *c*-axis at $B = 0$ [10, 11]. The turn angle of the helix is about 70° [12]. Magnetic measurements of $\text{Ba}_2\text{Mg}_2\text{Fe}_{12}\text{O}_{22}$ single crystals have demonstrated the possibility of a transition to the longitudinal-conical spin state below about 50 K [13]; the prospects of applications as a multiferroic material prompted extensive studies of the structural, magnetic and ferroelectric properties of single crystals of $\text{Ba}_2\text{Mg}_2\text{Fe}_{12}\text{O}_{22}$ [2, 13-17]. However, the properties of powder $\text{Ba}_2\text{Mg}_2\text{Fe}_{12}\text{O}_{22}$ have not been sufficiently explored. One of the reasons is that preparing a single-phase sample is very difficult, as is the case with most complex hexaferrites. The process of synthesizing Y-type hexaferrites always involves the presence of various accompanying magnetic oxides, the main cause of this being the fact that the temperature interval for Y-phase synthesis is very narrow. Typically, the Y-type hexaferrite phase synthesis begins at 900°C and ends at 1200°C . R. Pullar [18] provided a detailed study on the processes of hexaferrites synthesis. In brief, at the beginning, the preparation of $\text{Ba}_2\text{Mg}_2\text{Fe}_{12}\text{O}_{22}$ is accompanied by the presence of another type of hexaferrite, namely, M-type barium hexaferrite and of small amounts of second phases of barium ferrite and magnesium ferrite. A Z-type hexaferrite appears at temperatures above 1200°C . The type of the second phases present depends to a large extent on the type of Me cations and the preparation technique. This is why when one studies Y-type hexaferrites one should bear in mind the existence of second phases that may influence the material's multiferroic properties, so that this type of multiferroics should be considered as being natural composite materials.

We will consider here the structural and magnetic properties of $\text{Ba}_2\text{Mg}_2\text{Fe}_{12}\text{O}_{22}$ powders synthesized by sol-gel auto-combustion and by co-precipitation. In the case of $\text{Ba}_2\text{Mg}_2\text{Fe}_{12}\text{O}_{22}$ prepared by means of these two techniques, the second phase is MgFe_2O_4 . Studying the magnetic characteristics of MgFe_2O_4 is important, since its presence may affect the magneto-electric properties of the composite.

Magnesium ferrite has a cubic structure of the normal spinel-type (AB_2O_4) and is a soft magnetic n-type semiconducting materials [19, 20]. The general formula of magnesium ferrite could be written as $(\text{Mg}_{1-x}\text{Fe}_x)_\text{A}[\text{Mg}_x\text{Fe}_{2-x}]_\text{B}\text{O}_4$, where x is the inversion parameter and A and B are respectively the tetrahedral and octahedral position occupied by the Mg^{2+} and Fe^{3+} cations [21]. The Mg^{2+} and Fe^{3+} cations do not exhibit preference for any site in the spinel structure [22, 23]. The Curie temperature of magnesium ferrite is very sensitive to the intracrystalline distribution of Fe^{3+} and Mg^{2+} cations between tetrahedral and octahedral sites and falls within the interval 593 - 713 K [24, 25].

Together with presenting the results of the structural and magnetic measurements of the composite $\text{Ba}_2\text{Mg}_2\text{Fe}_{12}\text{O}_{22}$ and MgFe_2O_4 material produced, we will also report the results of studying a single-phase magnesium ferrite sample in an attempt to clarify its impact on the composite samples' multiferroic properties.

2. MATERIALS AND METHODS

2.1. $\text{Ba}_2\text{Mg}_2\text{Fe}_{12}\text{O}_{22}$ Synthesized by Auto-Combustion

The $\text{Ba}_2\text{Mg}_2\text{Fe}_{12}\text{O}_{22}$ powders were prepared following the citric acid sol-gel auto-combustion method. The corresponding metal nitrates were used as starting materials. A citric acid solution was slowly added to the mixed solution of nitrates as a chelator. The solution was slowly evaporated to form a gel. This gel was dehydrated at 120°C to obtain the barium-magnesium-iron citrate precursor. During the dehydration process, the gel turned into a fluffy mass and was burnt in a self-propagating combustion manner. During auto-combustion, the burning gel expanded rapidly in volume. The auto-combusted powders were annealed at 1170°C in air.

2.2. $\text{Ba}_2\text{Mg}_2\text{Fe}_{12}\text{O}_{22}$ Synthesized by Co-Precipitation

Stoichiometric amounts of $\text{Ba}(\text{NO}_3)_2$, $\text{Fe}(\text{NO}_3)_3$ and $\text{Mg}(\text{NO}_3)_2$ were dissolved in deionized water and, after homogenization, the co-precipitation process was initiated by adding NaOH at $\text{pH} = 11.5$. High power ultrasound stirring was applied to assist this process, which, as it is known, enhances the reaction rate, the mass transport and the thermal effects [26]. The high-power ultrasound was applied for 15 min, pulse on: 2 s, pulse off: 2 s, amplitude 40%. The ultrasonic processor used was Sonics, 750W. The precursors were calcined at 1170°C to obtain the $\text{Ba}_2\text{Mg}_2\text{Fe}_{12}\text{O}_{22}$ powder.

2.3. MgFe_2O_4 synthesized by auto-combustion

$\text{Fe}(\text{NO}_3)_3 \cdot 9\text{H}_2\text{O}$, $\text{Mg}(\text{NO}_3)_2 \cdot 6\text{H}_2\text{O}$ and citric acid (all with analytical-grade purity) were used as starting materials. The molar ratio of metal nitrates to citric acid was fixed at 1:3. The metal nitrates were dissolved together in a minimum amount of deionized water to get a clear solution. A citric acid solution was slowly added to the mixed solution of nitrates as a chelating agent. The solution was slowly evaporated to form a gel. This gel

was dehydrated at 120°C to obtain the magnesium-iron citrate precursor. During the dehydration process, the gel turned into a fluffy mass and was burnt in a self-propagating combustion manner. The as prepared auto-combusted powders were annealed at temperature 1100°C to obtain MgFe₂O₄.

The Ba₂Mg₂Fe₁₂O₂₂ and MgFe₂O₄ powders were characterized using X-ray diffraction analysis with Cu-K_α radiation and scanning electron microscopy (Philips ESEM XL30 FEG). The hysteresis measurements were carried out by a SQUID Quantum Design magnetometer at 4.2 K and at room temperature. The ZFC and FC measurements at a magnetic field of 100 Oe were performed on an Oxford Design 7000 susceptometer. The *ac*-magnetization was measured in an *ac*-magnetic field with amplitude of 10 Oe and frequency of 1000 Hz while the temperature was slowly raised (0.05 K/min).

3. RESULTS AND DISCUSSION

Unlike the preparation of pure BaFe₁₂O₁₉ (M-type hexaferrite) using the citrate precursor method, the Y-type phase powder cannot be produced so easily due to the complexity of its structure, which imposes a progressive transformation through intermediate ferrites before achieving the final structure required. Our earlier investigations [27] showed that at temperatures below 1170°C, Ba₂Mg₂Fe₁₂O₂₂ coexists with BaFe₂O₄ and MgFe₂O₄ phases. At temperatures above 1170°C, BaFe₂O₄ disappears and only a small amount of MgFe₂O₄ (less than 2 mass %) remains as a second phase. The XRD spectra of the powder obtained by co-precipitation showed the characteristic peaks corresponding to the Y-type hexaferrite structure (Ba₂Mg₂Fe₁₂O₂₂) as a main phase and to some MgFe₂O₄ impurity. Fig. (1) shows XRD spectra of Ba₂Mg₂Fe₁₂O₂₂ samples prepared by auto-combustion (a) and co-precipitation (b); MgFe₂O₄ powders after auto-combustion (c) and heat treatment at 1000°C (d).

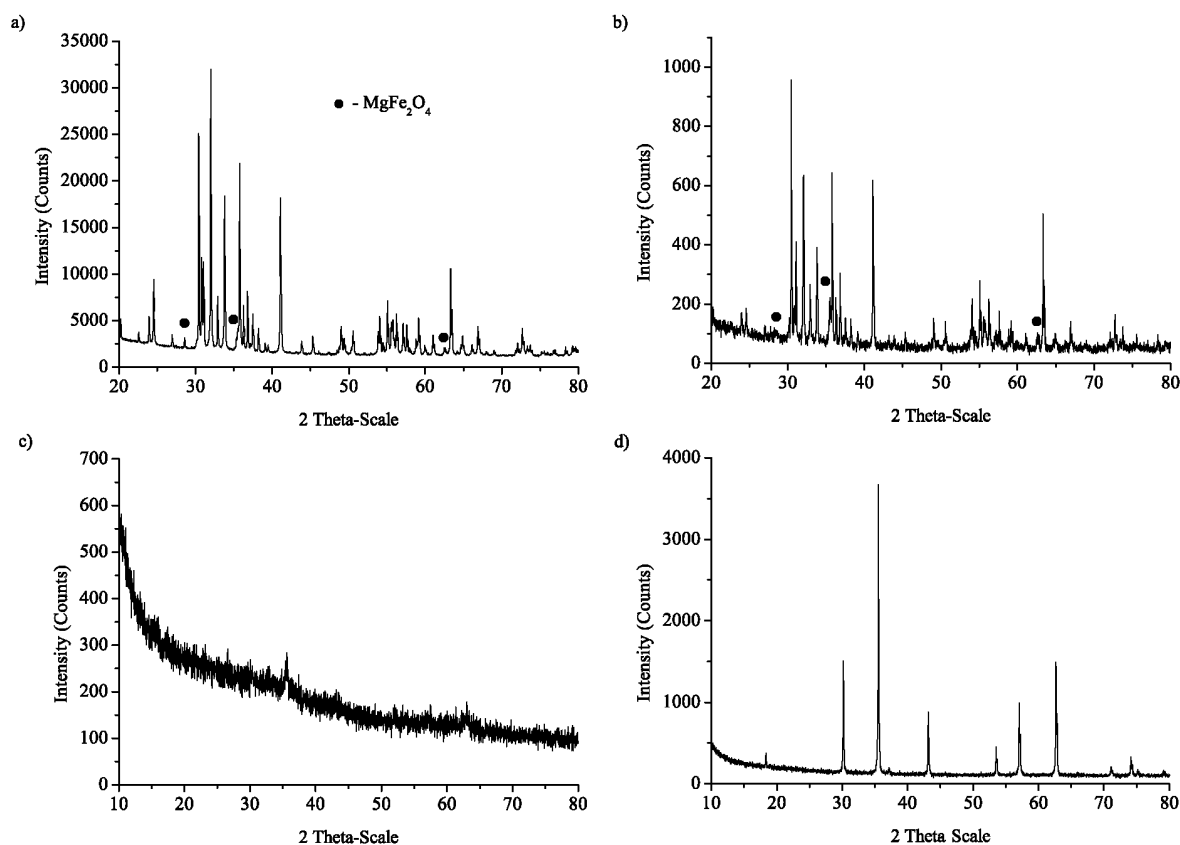


Fig. (1). XRD spectra of Ba₂Mg₂Fe₁₂O₂₂ samples prepared by auto-combustion (a) and co-precipitation (b); MgFe₂O₄ powders after auto-combustion (c) and heat treatment at 1000 °C (d).

The Rietveld refinement of the crystal structure of the $\text{Ba}_2\text{Mg}_2\text{Fe}_{12}\text{O}_{22}$ sample annealed at 1170°C revealed that, in contrast to the $\text{Ba}_2\text{Mg}_2\text{Fe}_{12}\text{O}_{22}$ structure where the Zn^{2+} cations occupy only tetrahedral cation positions, the Mg^{2+} cations are distributed over all cation positions leading to mixed occupancies of positions in the cation sublattice. The occupancies obtained are close to the corresponding values given by Momozawa *et al.* [10] for single-crystal $\text{Ba}_2\text{Mg}_2\text{Fe}_{12}\text{O}_{22}$. The Rietveld refinement confirmed a rhom-bohedral symmetry of the structure with unit cell parameters ($a = b = 5.8694(1) \text{ \AA}$ and $c = 43.4962(1) \text{ \AA}$; hexagonal setting). The unit cell parameters are in a good agreement with the values published earlier [10, 13].

XRD spectra of the MgFe_2O_4 powders after auto-combustion and heat-treatment are presented in (Fig. 1c, d). After auto-combustion, the material is predominantly amorphous. Small and broad peaks of MgFe_2O_4 and Fe_2O_3 (hematite) can be seen, indicating the poor crystalline state of the phases formed at this stage of the synthesis. The XRD spectrum of the sample synthesized at 1100°C shows the presence of MgFe_2O_4 only.

Scanning electron microscopy was used to examine the morphology of the samples. The SEM image of a $\text{Ba}_2\text{Mg}_2\text{Fe}_{12}\text{O}_{22}$ sample obtained by auto-combustion (Fig. 2a) shows that the particles are well agglomerated to form clusters of different sizes and shapes. Some of the clusters formed have a plate-like shape. The high degree of aggregation seen is due to the strong magnetic attraction forces. The SEM image of a $\text{Ba}_2\text{Mg}_2\text{Fe}_{12}\text{O}_{22}$ sample obtained by co-precipitation (Fig. 2b) shows that the particles have an almost perfect hexagonal shape. The powder consists almost entirely of large hexaferrite-phase particles with size of a few microns and of small MgFe_2O_4 particles. The average thickness of the $\text{Ba}_2\text{Mg}_2\text{Fe}_{12}\text{O}_{22}$ particles is 380 nm (Fig. 2c) is a TEM photograph of the small particles in the sample. The average particle size is about 20 nm . Fig. (2d) presents the growth of the separate hexagonal particles along the c axis; one can clearly see the successive stages of the $\text{Ba}_2\text{Mg}_2\text{Fe}_{12}\text{O}_{22}$ hexagonal particles growth. One can also see that some of the hexagonal particles are co-grown, which is more characteristic for bulk samples. This suggests that the precursor produced by co-precipitation can be applied to the preparation of bulk $\text{Ba}_2\text{Mg}_2\text{Fe}_{12}\text{O}_{22}$ samples of high density, such as targets for thin and thick films deposition. Furthermore, the well-shaped hexagonal particles are suitable for exploring these materials' fine crystal and magnetic structures.

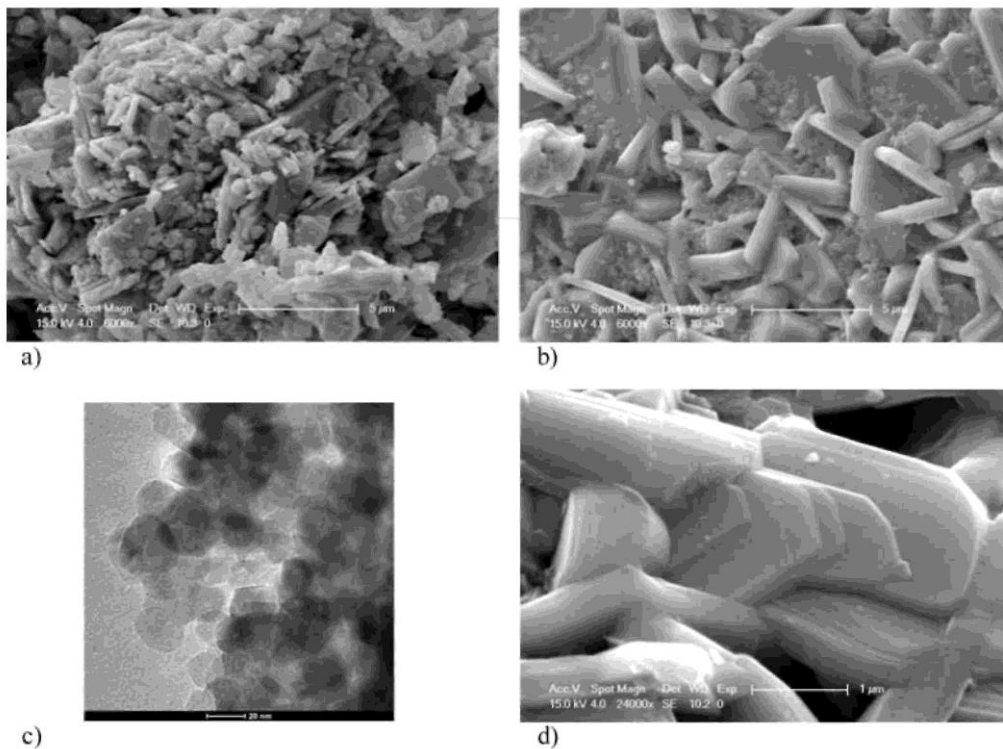


Fig. (2). SEM images of $\text{Ba}_2\text{Mg}_2\text{Fe}_{12}\text{O}_{22}$ powder obtained by auto-combustion (a) and co-precipitation (b, d). TEM image of MgFe_2O_4 in the powder obtained by co-precipitation (c).

Fig. (3a) shows an SEM image of the magnesium ferrite sample obtained by auto-combustion and annealed at 1100°C. The sample is homogeneous with respect to the particles size and shape. It is also seen that the particles have an approximately spherical shape. Fig. (3b) shows a TEM image of the MgFe_2O_4 powder. The particles are agglomerated to a large extent due to their small size and the magnetic attraction.

The hysteresis loops of the powder at room temperature and at 4.2 K are shown in (Fig. 4). The magnetic parameters, namely, the magnetization at 60 kOe, the remanent magnetization (M_r) and the coercivity field (H_c) obtained from the curves are listed in Table 1. The value of the magnetization M at 60 kOe for the sample prepared by co-precipitation is somewhat higher than that of the sample produced by auto-combustion. This is due to the well-expressed hexagonal shape of the particles and to their size (several microns). The value of H_c is low, which is typical for the hexaferrites with planar magneto-crystalline anisotropy. The sample prepared by auto-combustion contains a fraction of fine particles in a monodomain state; furthermore, the particles are well separated as compared with the sample produced by co-precipitation. These factors influence strongly the sample's magnetic properties at low temperatures, which is expressed as a significant increase of the coercivity field. The insets in Fig. (4a) and c show triple hysteresis loops at 4.2 K in a low-magnetic-field range indicating the presence of two kinds of ferromagnetic states with different magnetization values.

The magnetic phase-transitions were investigated in an *ac* magnetic field. The phase-transition temperatures were determined by following the variation of the powder's *ac* differential magnetization as the temperature was raised in an *ac* magnetic field with frequency 1000 Hz and amplitude 10 Oe (Fig. 5). The changes at 183 K for the sample obtained by auto-combustion and at 196 K for the sample obtained by co-precipitation are brought about by a phase transition from a ferromagnetic state to a spiral spin order state. This transition determines the multiferroic properties $\text{Ba}_2\text{Mg}_2\text{Fe}_{12}\text{O}_{22}$. The transitions at 40 K and 30 K for the sample obtained by auto-combustion and co-precipitation respectively are related to a spin reorientation along the *c* axis into a longitudinal conical state. The difference in the values of these transitions for the two samples is due to the differences in the particles' size and shape, as well as to the powder particles' orientation in the magnetic field applied. In comparison, the values of these transitions for single-crystal samples are 195 K and 50 K, respectively [28].

Fig. (6) presents the real (M) part of the *ac* magnetization. It does not exhibit any transitions, which indicates that the MgFe_2O_4 phase should not affect the magneto-electric properties of composite structures containing the Y-type hexaferrite $\text{Ba}_2\text{Mg}_2\text{Fe}_{12}\text{O}_{22}$ and less than 2 mass% of MgFe_2O_4 .

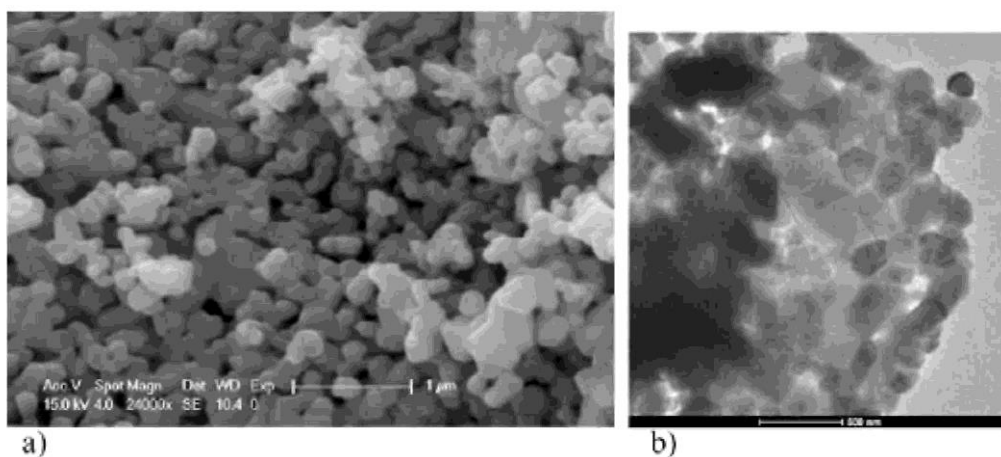


Fig. (3). SEM and TEM images of MgFe_2O_4 obtained by auto-combustion.

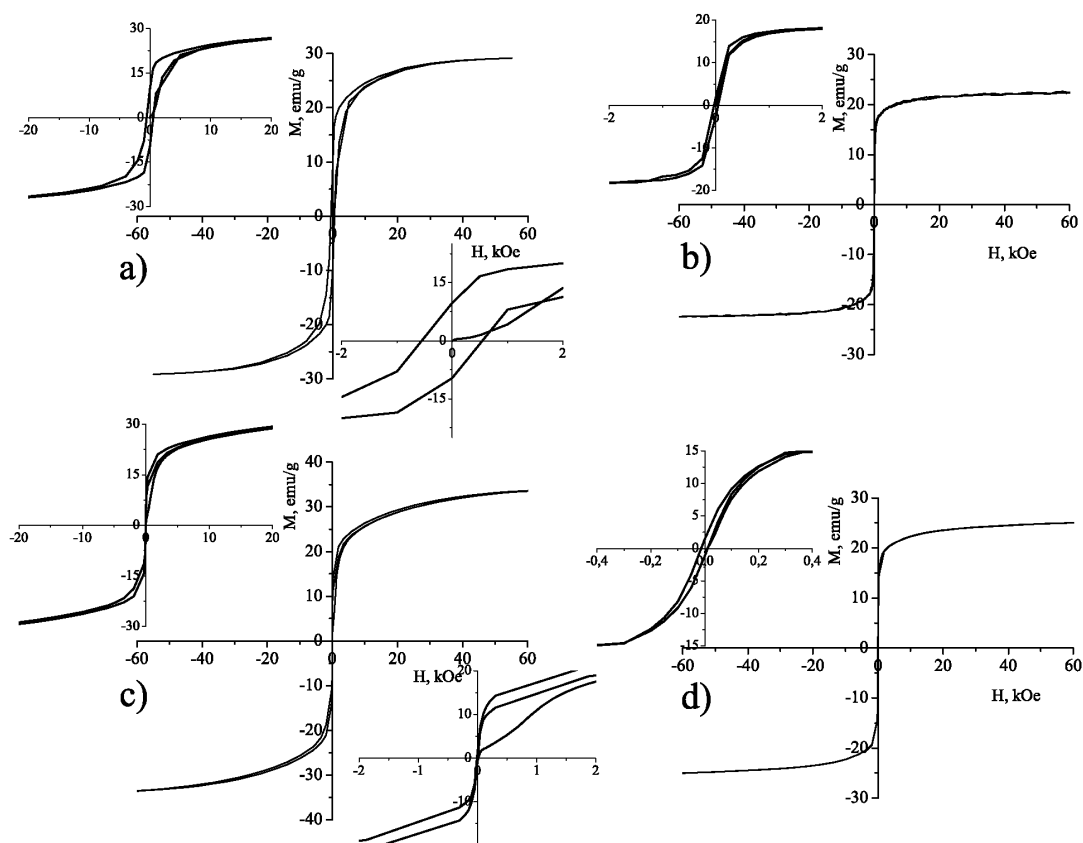


Fig. (4). Magnetic measurements of $Ba_2Mg_2Fe_{12}O_{22}$ powder obtained by auto-combustion (a, b) and co-precipitation (c, d) at 4.2 K (a, c) and 300 K (b, d).

Table 1. Magnetic properties of $Ba_2Mg_2Fe_{12}O_{22}$ powder synthesized at 1170°C for 5 h.

Sample	T, K	M(60kOe), emu/g	M_r , emu/g	H_c , Oe
$Ba_2Mg_2Fe_{12}O_{22}$ auto-combustion	300	22.78	1.74	31.35
$Ba_2Mg_2Fe_{12}O_{22}$ auto-combustion	4.2	30.47	9.69	545.87
$Ba_2Mg_2Fe_{12}O_{22}$ co-precipitation	300	24.95	1.26	12.21
$Ba_2Mg_2Fe_{12}O_{22}$ co-precipitation	4.2	33.57	1.94	28.95

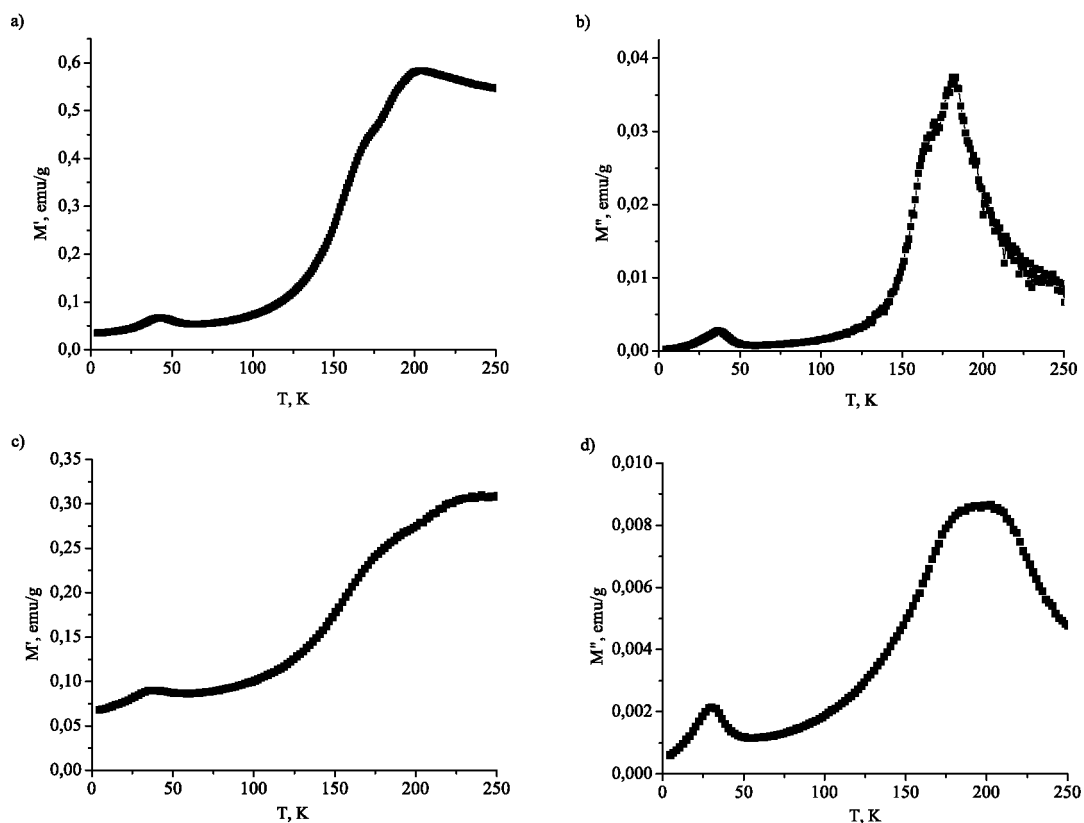


Fig. (5). Temperature dependence of the ac differential magnetization of $Ba_2Mg_2Fe_{12}O_{22}$ in an ac magnetic field with amplitude 10 Oe and frequency 1000 Hz: $M'(T)$ is the real part of the differential magnetization; $M''(T)$ is the imaginary part of the differential magnetization, a) for a sample obtained by auto-combustion; b) for a sample obtained by co-precipitation.

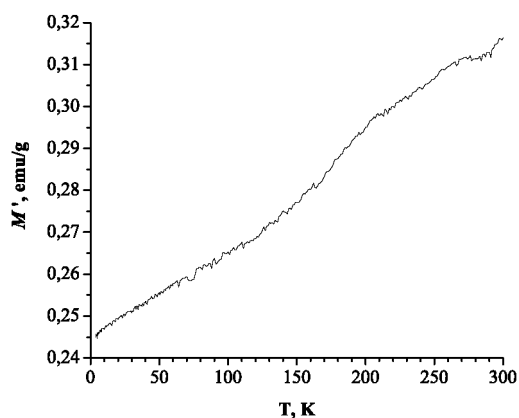


Fig. (6). ac magnetization $MgFe_2O_4$ in an ac field with amplitude 10 Oe and frequency 1 kHz.

CONCLUSION

We studied natural composite materials based on a Y-type hexaferrite $Ba_2Mg_2Fe_{12}O_{22}$ powder, which also included a second phase of $MgFe_2O_4$. The two techniques used to prepare the powder samples, namely, auto-combustion and co-precipitation, resulted in the formation of samples of different homogeneity with respect to

the particles' size, and to a different degree of sintering following an identical annealing process. The co-growth observed of the hexagonal particles in the sample obtained by co-precipitation makes this technique suitable for sintering of bulk materials. We observed two magnetic-phase transitions responsible for this composite material's multiferroic properties. We further demonstrated that the MgFe_2O_4 phase present does not affect the magneto-electric properties of the samples studied.

REFERENCES

- [1] Cheong, S.-W.; Mostovoy, M. Multiferroics: a magnetic twist for ferroelectricity. *Nat. Mater.*, 2007, 6, 13-20.
- [2] Taniguchi, K.; Abe, N.; Ohtani, S.; Umetsu, H.; Arima, T. Ferroelectric polarization reversal by a magnetic field in multiferroic Y-type hexaferrite $\text{Ba}_2\text{Mg}_2\text{Fe}_{12}\text{O}_{22}$. *Appl. Phys. Express*, 2008, 1, 031301.
- [3] Vaz, C.; Hoffman, J.; Ahn, Ch.; Ramesh, R. Magnetolectric coupling effect in multiferroic complex oxides composite structures. *Adv. Mat.*, 2010, 22, 2900-2918.
- [4] Kimura, T. Magnetolectric hexaferrites. *Annu Rev. Condens. Matter Phys.*, 2012, 3, 93-110.
- [5] Chun, S.; Chai, Y.; Oh, Y.; Jaiswal-Nagar, D.; Haam, S.; Kim, I.; Lee, B.; Nam, D.; Ko, K.; Park, J.; Chung, J.; Kim, K. Realization of giant magnetolectricity in Helimagnets. *Phys. Rev. Lett.*, 2010, 104, 037204.
- [6] Bai, Y.; Zhou, J.; Gui, Zh.; Li, L. Magnetic properties of Cu, Zn-modified CO_2Y hexaferrite. *J. Magn. Magn. Mater.*, 2002, 246, 140-144.
- [7] Zuo, Xu; How, H.; Shi, P.; Oliver, S.A.; Vittoria, C. Zn_2Y hexaferrite ($\text{Ba}_2\text{Mg}_2\text{Fe}_{12}\text{O}_{22}$) single-crystal microstripline phase shifter. *IEEE Trans. Magn.*, 2002, 38, 3493-3497.
- [8] Temujin, J.; Aoyama, M.; Senna, M.; Masuko, T.; Ando, C; Kishi, H. Synthesis of Y-type hexaferrite via a soft mechanochemical route. *J. Solid State Chem.*, 2004, 177, 3903-3908.
- [9] Kamishima, K.; Ito, C; Kakizaki, K.; Hiratsuka, N.; Shirahata, T.; Imakubo, T. Improvement of initial permeability for Z-type ferrite by Ti and Zn substitution. *J. Magn. Magn. Mater.*, 2007, 312, 228-233.
- [10] Momozava, N.; Yamaguchi, Y.; Mita, M. Magnetic structure change in $\text{Ba}_2\text{Mg}_2\text{Fe}_{12}\text{O}_{22}$. *J. Phys. Soc. Jpn.*, 1986, 55, 1350-1358.
- [11] Nakamura, S.; Tsunoda, Y.; Fuwa A. Moesbauer Study on Y-type hexaferrite $\text{Ba}_2\text{Mg}_2\text{Fe}_{12}\text{O}_{22}$. *Hyperfine Interact.*, 2012, 208, 49-52.
- [12] Tokura, Y.; Seki, S. Multiferroics with spiral spin orders. *Adv. Mater.*, 2010, 22, 1554-1565.
- [13] Ishiwata, S.; Okuyama, D.; Kakurai, K.; Nishi, M.; Taguchi, Y.; Tokura, Y.; Neutron diffraction studies on the multiferroic conical magnet $\text{Ba}_2\text{Mg}_2\text{Fe}_{12}\text{O}_{22}$. *Phys. Rev. B.*, 2010, 81, 174418.
- [14] Ishiwata, S.; Taguchi, Y.; Murakawa, H.; Onose, Y.; Tokura Y. Low-magnetic-field control of electric polarization vector in a helimagnet. *Science*, 2008, 319, 1643-1646.
- [15] Kida, N.; Okuyama, D.; Ishiwata, S.; Taguchi, Y.; Shimano, R.; Iwasa, K.; Arima, T.; Tokura, Y. Electric-dipole-active magnetic resonance in the conical-spin magnet $\text{Ba}_2\text{Mg}_2\text{Fe}_{12}\text{O}_{22}$. *Phys. Rev. B.*, 2009, 80, 220406(R).
- [16] Sagayama, H.; Taniguchi, K.; Abe, N.; Arima, T.; Nishikawa, Y.; Yano, S.; Kousaka, Y.; Akimitsu, J.; Matsuura, M.; Hirota, K. Two distinct ferroelectric phases in the multiferroic Y-type hexaferrite $\text{Ba}_2\text{Mg}_2\text{Fe}_{12}\text{O}_{22}$. *Phys. Rev. B.*, 2009, 80, 180419(R).
- [17] Ishiwata, S.; Taguchi, Y.; Murakawa, H.; Onose, Y.; Tokura, Y. Magnetic-field control of electric polarization in a helimagnetic hexaferrite $\text{Ba}_2\text{Mg}_2\text{Fe}_{12}\text{O}_{22}$. *J. Phys. Condens. Matter*, 2009, 21, 042073.
- [18] Pullar, R.C. Hexagonal ferrites: A review of the synthesis, properties and applications of hexaferrite ceramics. *Prog. Mater. Sci.*, 2012, 57, 1191-1334.
- [19] Ahmed, Y.M.Z.; Ewais, E.M.M.; Zaki, Z.I. In situ synthesis of high density magnetic ferrite spinel (MgFe_2O_4) compacts using a mixture of conventional raw materials and waste iron oxide. *J. Alloys Compd.*, 2010, 489, 269-274.
- [20] Maensiri, S.; Sangmanee, M; Wiengmoon, A. Magnesium ferrite (MgFe_2O_4) nanostructures fabricated by electrospinning. *Nanoscale Res. Lett.*, 2009, 221-228.
- [21] Antic, B.; Jovic, N.; Pavlovic, M.B.; Kremenovic, A.; Manojlovi, D. Magnetization enhancement in nanostructured random type MgFe_2O_4 spinel prepared by soft mechanochemical route. *J. Appl. Phys.*, 2010, 707, 043525.
- [22] Navrotsky, A.; Kleppa, J.O. The thermodynamics of cation distributions in simple spinels. *J. Inorg. Nucl. Chem.*, 1967, 29, 2701-2714.
- [23] Gateshki, M.; Petkov, V.; Pradhan, S.; Vogt T. Structure of nanocrystalline MgFe_2O_4 from X-ray diffraction, Rietveld and atomic pair distribution function analysis. *J. Appl. Crystallogr.*, 2005, 38, 772-779.

[24] Harrison, R.J.; Putnis, A. Determination of the mechanism of cation ordering in magnesioferrite (MgFe_2O_4) from the time- and temperature-dependence of magnetic susceptibility. *Phys. Chem. Miner.*, 1999, 26, 322-332.

[25] Rane, K.S.; Verenkar, V.M.S.; Sawant P.Y. Dielectric behaviour of MgFe_2O_4 prepared from chemically beneficiated iron ore rejects. *Bull. Mater. Sci.*, 2001, 24, 323-330.

[26] Manickam, S.; Rana, R. K. In: *Ultrasound Technologies for Food and Bioprocessing*; Feng, H.; Barbosa-Canovas, G.; Weiss, J., Eds.; Food Engineering Series, Springer Science+Business Media, LLC, 2011, pp. 405-444.

[27] Koutzarova, T.; Kolev, S.; Nedkov, I.; Krezhov, K.; Kovacheva, D.; Blagoev, B.; Ghelev, Ch.; Henrist, C; Cloots, R.; Zaleski, A. Magnetic properties of nanosized $\text{Ba}_2\text{Mg}_2\text{Fe}_2\text{O}_{22}$ powders obtained by auto-combustion. *J. Supercond. Novel Magn.*, 2011, 25(8), 2631-2635.

[28] Kida, N.; Kumakura, S.; Ishiwata, S.; Taguchi, Y.; Tokura Y. Gigantic terahertz magnetochromism via electromagnons in the hexaferrite magnet $\text{Ba}_2\text{Mg}_2\text{Fe}_2\text{O}_{22}$. *Phys. Rev. B.*, 2011, 83, 064422.